Atom Indonesia

Dosimetric Evaluation of Very High Energy Electron (VHEE) Beams in the Male Pelvic Region Using Geant4/TOPAS

E. M. Essaidi[1*], M. Krim[1], O. Kaanouch[1], M. Tantaoui[2], M. R. Mesradi[1], A. Didi[1], D. Benchekroun[3]

[1] Laboratory of Sciences and Health Technologies, High Institute of Health Sciences, Hassan First University of Settat, BP 555, Settat, 26000, Morocco
[2]Subatomic Research and Applications Team, Laboratory of the Physics of Condensed Matter (LPMC-ERSA), Faculty of Sciences Ben M'Sik, Hassan II University, BP 7955, Casablanca, 20023, Morocco
[3]Laboratory of High Energy Physics and Condensed Matter, Department of Physics,Faculty of Sciences Aïn Chock, Hassan II University, Casablanca, 20023, Morocco

A R T I C L E   I N F O

A B S T R A C T

The CLEAR (CERN Linear Electron Accelerator for Research) facility has significantly advanced high-energy electron radiotherapy, particularly for treating deep-seated tumors. However, achieving precise and accessible treatment delivery while minimizing damage to surrounding healthy tissues remains challenging. Very High Energy Electrons Beam (VHEE) offer notable potential due to their deep penetration capabilities. However, their nearly uniform dose distribution raises concerns about unintended exposure to healthy tissues. A key innovation in this field is the use of focused VHEE beams, which deliver a concentrated dose to a small defined area at a high dose rate, potentially enhancing treatment precision. This study evaluates the dosimetric characteristics of focused VHEE beams compared to collimated beams using GEANT4/TOPAS Monte Carlo simulations. A beamline with two quadrupole magnet triplets was designed to focus VHEE beams on a water phantom, simulating clinical conditions. The findings show that focused VHEE beams increased the dose to the prostate by 5.24 % while significantly reducing the dose to adjacent organs at risk: 16.93 % to the bladder, 50.81 % to the rectum, and 68.75 % to the femoral heads. These reductions highlight the dosimetric advantage of focused VHEE beams in sparing non-targeted tissues. While these results underscore the potential benefits of focused VHEE beams for deep-seated tumor treatment, additional research, including clinical validation and patient-specific modeling, is essential to fully evaluate their clinical utility. This study lays the groundwork for optimizing VHEE beam applications in cancer therapy by demonstrating improved dose delivery accuracy and reduced risk to adjacent organs.

INTRODUCTION

The commissioning of the CERN Linear Electron Accelerator for Research (CLEAR) marks a significant milestone in medical physics and accelerator technology, building on the foundation of the Advanced Proton Driven Plasma Wakefield Acceleration Experiment (AWAKE). Developed from the CLIC Test Facility 3 (CTF3), CLEAR became operational in 2017 with the goal of advancing research in accelerator development, high-gradient acceleration, beam instrumentation, and medical applications such as FLASH radiotherapy and dosimetry.

Very High Energy Electron (VHEE) beams, with energies of 200 MeV were first investigated for radiotherapy by Poppinga et al. in 2020, focusing on their potential for ultra-high dose rate conditions and the treatment of deep-seated tumors [1]. Subsequent studies further demonstrated their effectiveness in targeting tumors located in highly heterogeneous and mobile tissues [2]. VHEE radiotherapy offers several advantages over traditional external beam

radiotherapy, including deeper dose penetration, improved dose conformity, higher dose rates, and the ability for magnetic beam steering [3,4]. Additionally, the development of C-band radio-frequency (RF) accelerators and Laser Wake-Field Accelerators (LWFA) is expected to expand the availability of VHEE sources [5,6].

Despite these advantages, VHEE beams pose certain challenges, particularly their quasi-uniform dose distribution along the beam path, which may result in unnecessary exposure to healthy tissues [7]. Addressing these challenges requires innovative solutions to enhance dose delivery while minimizing collateral effects. The introduction of focused VHEE beams presents a promising approach by concentrating the dose within a small, well-defined region at a high dose rate [8]. The use of quadrupole magnets to focus VHEE beams has been shown to improve dose distribution by reducing entrance dose and enhancing precision in water phantoms [7,9].

Several studies have further explored the clinical applications and advantages of VHEE beams in radiotherapy. Foundational research highlighted the potential of 200 MeV electron beams for cancer treatment under ultra-high dose rate conditions [1], while other work provided a comprehensive overview of the characteristics of very high-energy electron beams for the irradiation of deep-seated targets [10]. Monte Carlo simulations have illustrated the feasibility of using laser-plasma accelerators for radiotherapy [11], and have demonstrated the potential of high-energy electron radiotherapy using a laser-accelerated beam prototype, including experimental tumor control in mice [12]. Further studies demonstrated the potential of VHEE beams delivered at FLASH dose rates for treating deep-seated tumors, with a specific focus on prostate cancer [13]. In various areas, extensive work has been conducted using Monte Carlo simulations to investigate underlying physical principles and achieve objectives aimed at improving treatment outcomes [14-16].

To provide further examples of the application of VHEE beam technology, studies have explored its use in prostate cancer treatment [4], as well as the development of laser-driven VHEE beams for radiotherapy [6]. Comparisons between VHEE and VMAT plans have shown that VHEE offers superior dose distribution [8]. Investigations into multi-field and intensity-modulated strategies for laser-driven VHEE therapy have highlighted their potential for optimizing treatment delivery [6]. Additionally, focused VHEE beams have been introduced as a novel modality, demonstrating the capability to achieve precise and highly accurate dose delivery [17].

This study presents the design and implementation of a beamline using two quadrupole magnet triplets to focus VHEE beams on a water phantom. It compares the dose deposition characteristics of focused versus collimated VHEE beams, highlighting the superior performance of focused beams in targeting deep-seated tumors. The results demonstrate that focused VHEE beams significantly enhance targeting precision while reducing doses to nearby organs, offering improved safety for patients and protection for healthcare personnel. A dosimetric comparison applied to the male pelvic region, modeled using a mathematical phantom with realistic dimensions in GEANT4/TOPAS Monte Carlo simulations, further underscores the clinical potential of focused VHEE beams in minimizing doses to organs at risk.

METHODOLOGY

This study investigates the dose deposition characteristics of focused VHEE beams in comparison to collimated VHEE beams using the TOPAS Monte Carlo simulation toolkit, which serves as an advanced interface for the GEANT4 toolkit [18-20]. The primary objective was to design and optimize a beam line tailored for VHEE therapy, emphasizing precision in targeting tumor sites while minimizing exposure to surrounding healthy tissues.

Monte Carlo simulation configurations

Simulation studies comparing focused VHEE beams to collimated VHEE beams were performed using the TOPAS (Tool for PArticle Simulation) Monte Carlo code. TOPAS, a user-friendly interface for the GEANT4 Monte Carlo simulation toolkit, facilitates the modeling of particle transport through matter using an object-oriented C++ framework. The physics list modules for radiotherapy simulations were selected based on prior research [20-22]. These modules, detailed in Table 1, were employed in the current simulations.

Table 1. Physics lists used in TOPAS simulations.

Physics List	Description
G4EmStandardPhysics_option4	Electromagnetic interactions
G4HadronElasticPhysics	Elastic hadronic physics
G4HadronElasticPhysics	Inelastic physics interactions for protons and neutrons
G4IonBinaryCascadePhysics	Inelastic interactions of other ions
G4EmExtraPhysics	Photo-nuclear processes
G4StoppingPhysics	Stopping power physics

110

The initial electron beam energy was set at 150 MeV with an energy spread of 0.75 MeV. Each simulation involved 1 million electrons incident on a water phantom modeled as a cuboid with dimensions of 30 × 30 × 30 cm³. This setup allowed for a detailed analysis of dose deposition characteristics under conditions representative of clinical scenarios.

The simulations were executed on the HPC-MARWAN platform using TOPAS (v7.3). High-performance computing resources were utilized to effectively handle the computational demands of large-scale simulations. Challenges associated with processing and resource management were addressed by optimizing the HPC workflow, ensuring reliable and robust simulation results.

Dose distribution and particle flux within the water phantom were evaluated using cuboid dose scoring meshes with a voxel size of 0.1 × 0.1 × 0.1 mm³. This scoring approach provided high spatial resolution, enabling precise quantification of dose deposition and flux within the phantom.

Pelvic anatomical model

To determine the dose delivered to the prostate and nearby organs at risk, a detailed model of the male pelvic region was developed. This model included the prostate, bladder, rectum, and both femoral heads, represented as a mathematical phantom with realistic dimensions and clinical data provided by O'Daniel et al. [23]. The anatomical structures were contained within an ellipsoidal tank with dimensions of 12 cm along the X-axis, 12 cm along the Y-axis, and 15 cm along the Z-axis (Figs. 1a and 1b). The tank was filled with water (H_2O), which was defined in GEANT4/TOPAS as G4_WATER, with a density of 1 g/cm³. The prostate was modeled as an ellipsoid using clinical data from ten patients, yielding average dimensions of approximately 5.01 cm in width, 3.49 cm in height, and 4 cm in thickness.

The prostate was modeled as an ellipsoid using clinical data from ten patients, yielding average dimensions of approximately 5.01 cm in width, 3.49 cm in height, and 4 cm in thickness. Prostate stones are mainly composed of calcium phosphates [24], consisting of 51.6 % calcium phosphates and calcium oxalates, 32.3 % pure calcium phosphates, 6.4 % pure calcium oxalates, 3.2 % sodium urate, 3.2 % brushite, and 3.2 % uric acid. For this study, the prostate was represented using calcium phosphate ($Ca_3(PO_4)_2$) with a density of 1.025 g/cm³, as noted by the Condensed Matter Chemistry Laboratory, Paris [24].

The bladder, modeled as an ellipsoid with dimensions of approximately 9.28 cm in width, 6.93 cm in height, and 4 cm in thickness, was also represented using water (H_2O) with a density of 1 g/cm³. The rectum was simplified as a torus and modeled with the material "G4_MUSCLE_STRIATED_ICRU" at a density of 1.04 g/cm³. Both femoral heads were modeled as torus structures using "G4_BONE_COMPACT_ICRU" at a density of 1.85 g/cm³.
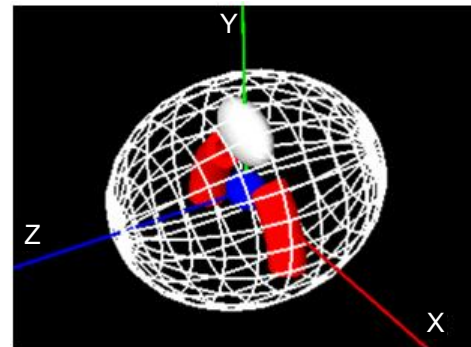
(a)
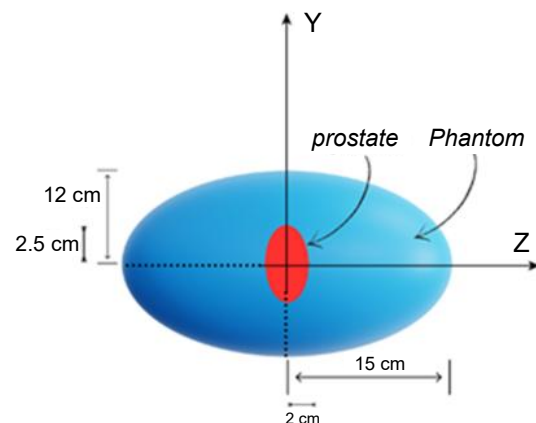
(b)

Fig. 1. (a) Visualization result of the male pelvic area using GEANT4/TOPAS and (b) Geometric structure of the model.

The decision to focus on the prostate as a model for this study was informed by previous research, including the work of cited in [25], which highlights the prostate's commonality as a cancer site and its anatomical relevance. The proximity of the prostate to critical structures such as the bladder and rectum makes it an appropriate model for examining the precise targeting capabilities of VHEE beams, as these surrounding organs are sensitive to radiation exposure. Accurate dose delivery to the prostate while sparing these critical organs is crucial for minimizing side effects and improving treatment outcomes.

Beam configuration and setup

For the collimated VHEE beam setup, an initial beam with a cross-section of 10 × 10 cm² was generated. This beam passed through a collimator with a central aperture of 5 cm diameter, embedded in a cylindrical structure with a total diameter of 15 cm. The collimator, constructed from G4_W (tungsten), was placed 40 cm downstream from the beam source. The water phantom was positioned 100 cm from the beam source.

This configuration effectively narrowed and concentrated the beam, significantly reducing lateral scattering. The collimated beam was directed at the water phantom to assess dose distribution and optimize treatment parameters, focusing on enhancing targeting precision while minimizing exposure to surrounding healthy tissues (Fig. 2a).

In the focused VHEE beam setup, an initial beam with a cross-section of 10 × 10 cm² first passed through three quadrupole defocusing magnets (QD1, QD2, QD3), positioned 30 cm from the beam source, to slightly spread the beam. This was followed by three quadrupole focusing magnets (QF4, QF5, QF6), positioned 60 cm from the beam source. The focused beam then continued from the final quadrupole (QF6) to the water phantom (Fig. 2b).
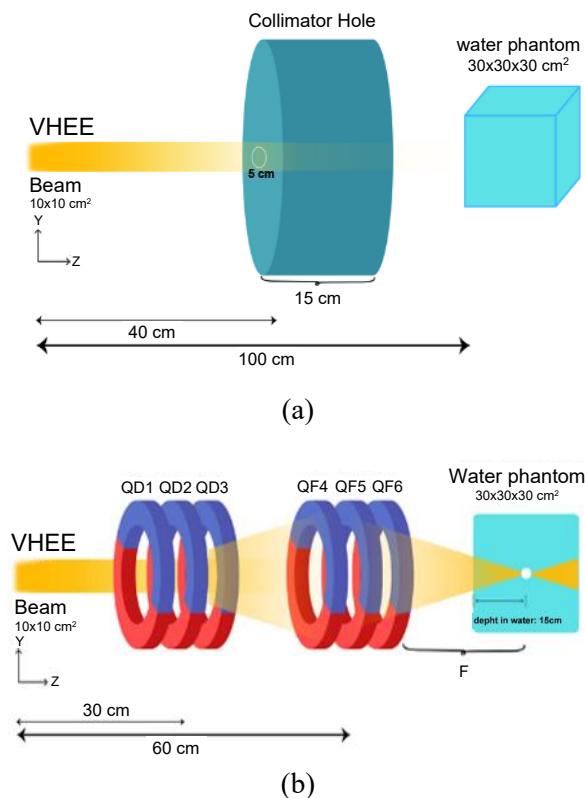
To achieve precise focusing, the quadrupole magnets exploit their linear magnetic field gradient, described by $Bx = \Gamma y$ and $By = \Gamma x$, where Γ is the magnetic field gradient. This gradient creates a restoring force on the electrons, proportional to their displacement, these terms as given by Eq. (1):

$$F = \frac{-q\Gamma v}{\gamma m} \times y \qquad (1)$$

where γ is the Lorentz factor. This force focuses the electron beam in one dimension while defocusing it in the orthogonal plane, necessitating careful quadrupole arrangements. The focal length ($z0$) of each quadrupole was calculated to align with the prostate depth, as given by Eq. (2):

$$z0 = \frac{\pi}{2} \frac{\gamma mc}{q\Gamma} \qquad (2)$$

To simplify the design, the thin-lens approximation was applied by Eq. (3):

$$f = \frac{1}{k\tan(kL)} \qquad (3)$$

where k explains with Eq. (4)

$$k = \sqrt{\frac{q\Gamma}{\gamma mc}} \qquad (4)$$

This approach allowed for optimal tuning of the quadrupoles QF4, QF5, QF6 to achieve a focal length of 15 cm along the Z-axis and 12 cm along the Y-axis, ensuring precise dose delivery to the prostate while minimizing exposure to surrounding organs.

The beam focusing system utilized two quadrupole groups: the defocusing group (QD1, QD2, QD3) to initially spread the beam, and the focusing group (QF4, QF5, QF6) to converge it precisely onto the target. This arrangement allowed for precise dose concentration at the tumor site while protecting healthy tissue. A smaller focal length value (F1 > F2) indicates a more precise and deeper beam focus, as detailed in Table 2.

(a)

(b)

Fig. 2. Schematic of the generation of VHEE beams (a) Collimated VHEE beam and (b) Focused VHEE beam.

Table 2. Parameters of the second group of quadrupoles with 150 MeV.

Depth in Water	Q4 Gradient [T/m]	Q5 Gradient [T/m]	Q6 Gradient [T/m]
F1 (12 cm)	(-9.79, 9.79)	(-9.98, 9.98)	(-11.23, 11.23)
F2 (15 cm)	(-9.79, 9.79)	(-9.98, 9.98)	(-11.23, 11.23)

Electron beams were emitted from a point source with predefined trajectories. Anterior and posterior beams (0° and 180°) were aligned along the Z-axis, while lateral beams (90° and 270°) were directed perpendicular to the Z-axis along the Y-axis. These beam orientations were selected to ensure comprehensive target coverage and optimal dose distribution, consistent with the methodology described by O'Daniel et al. (2010) [23].

In 3D Conformal Radiotherapy (3D-CRT), this configuration facilitates radiation delivery from multiple angles, reducing the dose to surrounding critical structures while enhancing dose uniformity within the prostate. Such an arrangement ensures a more conformal and homogeneous dose delivery to the target region. For all beam angles, the source-to-phantom prostate distance was fixed at 100 cm, enabling precise dose measurement at the prostate's center.

RESULTS AND DISCUSSION

The dosimetric characteristics of VHEE beams are illustrated through simulated Percentage Depth Dose (PDD) profiles, which compare the dose distributions of various beam types and energies within a water phantom. The study includes 18 MV photon beams, 150 MeV proton beams, and VHEE beams at 50 MeV, 150 MeV, and 250 MeV. The results presented in Fig. 3 illustrate the depth dose distribution characteristics of each beam type.
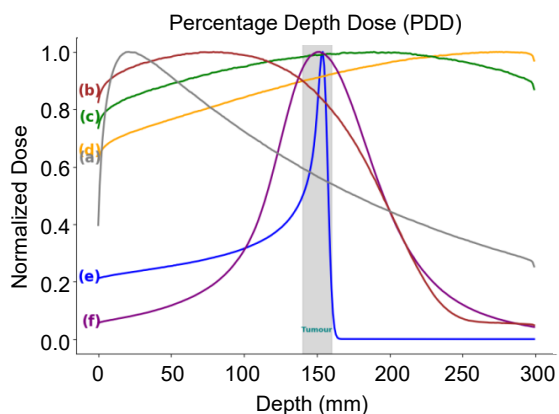

Fig. 3. Normalized Percentage Depth Dose (PDD) profiles for various radiation types and energies in a water phantom (a: 18 MV photons, b: Collimated 50 MeV electrons, c: Collimated 150 MeV electrons, d: Collimated 250 MeV electrons, e: Collimated 150 MeV protons-15cm, f: Focused 150 MeV electrons-15cm).

The 18 MV photon beam demonstrates a rapid dose falloff after a shallow penetration, concentrating the dose near the surface. This characteristic makes the photon beam effective for treating superficial tumors but less suitable for deep-seated tumors, as it risks overexposing the surrounding healthy tissues. In contrast, the collimated 50 MeV electron beam exhibits a more gradual dose falloff. While it does not penetrate as deeply as the higher energy VHEE beams, it is suitable for mid-depth tumor treatments, providing a more controlled dose distribution.

The 150 MeV collimated electron beam delivers a relatively uniform dose up to a significant depth before experiencing a sharp falloff. This makes it particularly useful for treating deep-seated tumors, ensuring that the dose is delivered effectively to the target while minimizing the risk of overexposure to surrounding tissues. The 250 MeV collimated electron beam penetrates even deeper, maintaining a consistent dose over a larger range, which is ideal for very deep tumors. This ensures adequate dose delivery to the tumor while sparing healthy tissues around the tumor site.

In comparison, the 150 MeV proton beam displays the characteristic Bragg peak, which enables precise targeting of tumors at specific depths. The sharp rise and fall in dose associated with the Bragg peak allows for reduced exit doses, making protons particularly effective for treating tumors where precise depth control is required.

The focused 150 MeV electron beam shows a distinct dose peak at a specific depth, highlighting the benefits of focusing the beam. This approach enhances targeting precision, delivering higher doses directly to the tumor while minimizing the dose to surrounding healthy tissues. This technique is particularly advantageous for complex tumor geometries and locations, as it allows for more accurate and localized dose delivery.

These dose profiles demonstrate that VHEE beams, especially at higher energies, offer a promising alternative for radiotherapy. They provide deep penetration with controlled dose distribution, making them well-suited for targeting tumors located deep within the body while sparing surrounding non-cancerous tissues. Additionally, focused VHEE beams show great potential for precise dose delivery, which confirmed that focused VHEE beams can concentrate doses into small volumetric elements within a target [7]. The study demonstrated good agreement between measured dose distributions and Monte Carlo simulations, further supporting the use of focused VHEE beams in advanced radiotherapy.

The figure legend has been refined to clearly distinguish between collimated and focused beams, emphasizing their respective applications and showcasing the advantages of using focused VHEE beams for precise treatment planning.

The second part of the study focuses on simulating axial dose distributions for VHEE beams aimed at the prostate. The simulation involved two different depth settings: 12 cm at 90° and 270° angles, and 15 cm at 0° and 180° angles as shown in Fig. 4. The PDD curves show that the focused 150 MeV electron beam at 12 cm (green curve) and at 15 cm (orange curve) provide a distinct dose peak at their respective depths, indicating a concentrated dose at the tumor site as shown in Fig. 5. This is crucial for effectively targeting the prostate while minimizing the dose to surrounding healthy tissues. The collimated 150 MeV electron beam (blue curve) shows a more uniform dose distribution but lacks the precision of the focused beams, potentially increasing the risk of collateral damage. These findings align with previous studies that highlight the importance of using VHEE beams with energies greater than 100 MeV for deep-seated tumors [26]. This choice ensures sufficient penetration and dose concentration at the tumor site, enhancing treatment precision and efficacy for prostate tumors.
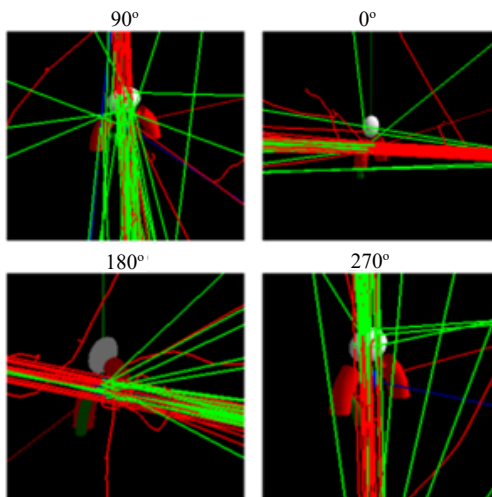

Fig. 4. Visualization of interactions at different angles: Simulation for prostate targeting
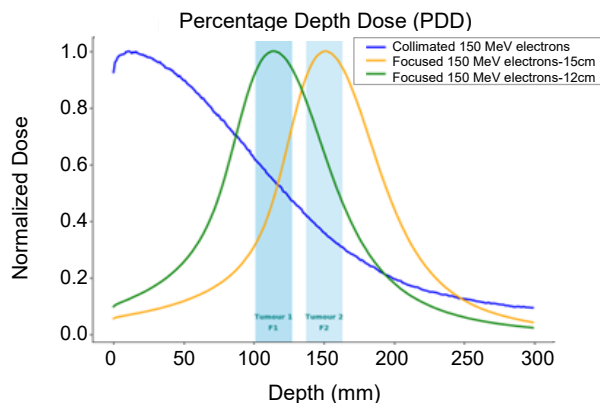(Red line: Electrons, green line: Photons).

Fig. 5. Simulating axial dose distributions for VHEE beams: Normalized Percentage Depth Dose (PDD) curves for collimated and focused 150 MeV electron beams.

Furthermore, the dose distributions for collimated and focused 150 MeV electron beams at different focus settings (F1 and F2) are compared, as shown in Fig. 6. The focused beam settings (F1 and F2) demonstrate a higher concentration of dose at specific depths compared to the collimated beam, which maintains a more uniform dose distribution. This comparison illustrates the enhanced precision and potential for reduced collateral damage with focused VHEE beams.
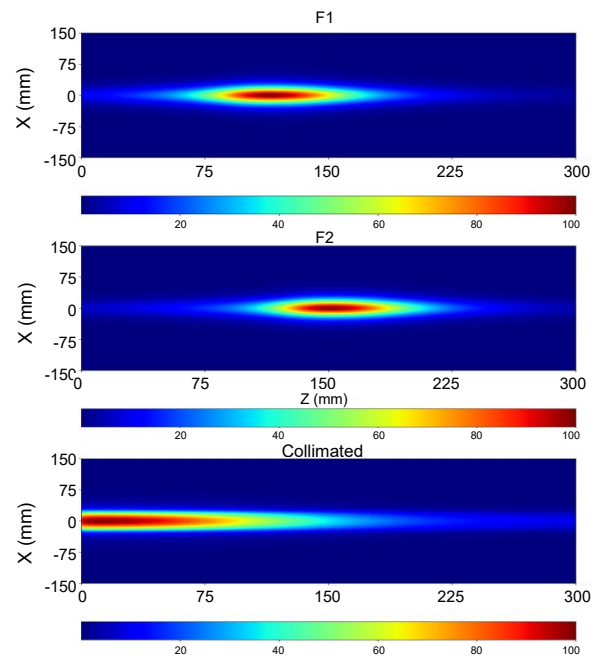

Fig. 6. Dose distributions for collimated and focused 150 MeV electron beams at different focus settings (F1 and F2).

The comparison of lateral scattering between collimated and focused VHEE beams show distinct dose distribution differences. Figures 4 and 6 highlight that collimated VHEE beams experience significant lateral scattering, resulting in a broader dose spread and potential exposure to surrounding adjacent tissues. In contrast, focused VHEE beams exhibit significantly reduced lateral scattering due to the use of quadrupole magnets [7,17]. These magnets precisely focus the electron beams by converting them into a smaller, well-defined spot, thus confining the electrons and minimizing their lateral spread. This decrease enables a more concentrated dose at the target depth, improving precision while minimizing exposure to adjacent tissues.

After simulating the pelvic male phantom and prostate, the study continued with simulations of 150 MeV collimated and focused VHEE beams. A total of 10^6 events were simulated for each setup. We then calculated the percentage of the deposited dose in the prostate and in the organs at risk to determine which particle allowed the minimum dose to be deposited in the organs at risk. The results are shown in Tables 3 and 4 and Fig. 7.
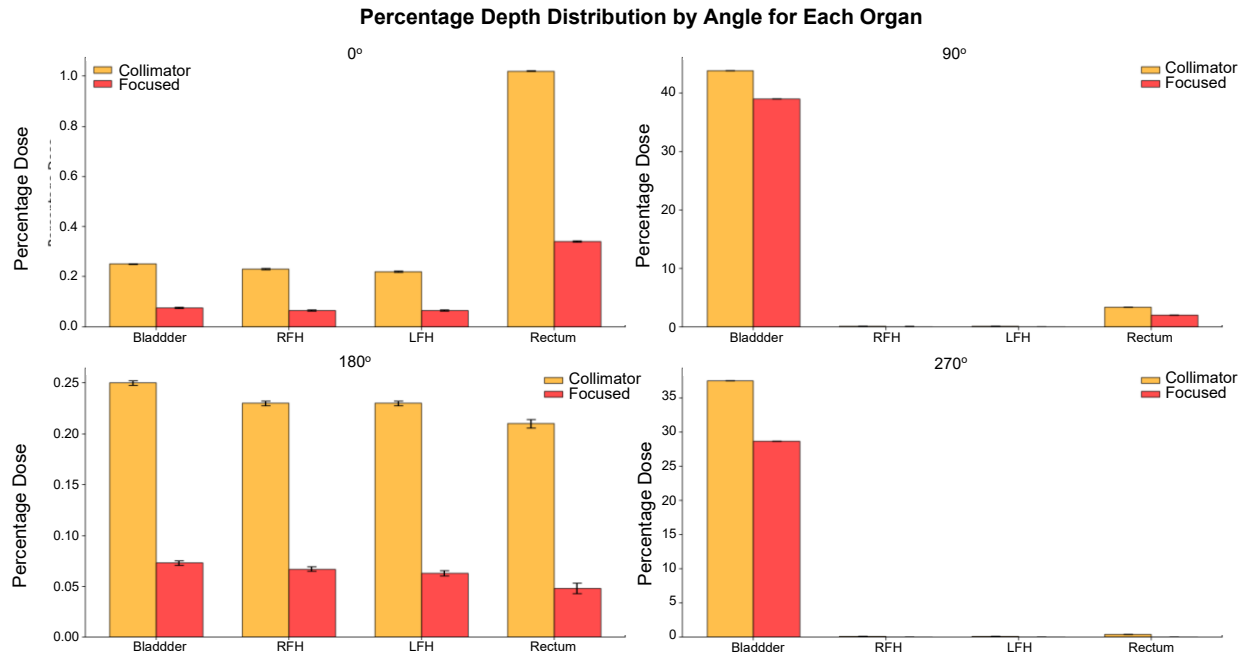
Percentage Depth Distribution by Angle for Each Organ

Fig. 7. Percentage dose distribution by angle for each organ in pelvic male prostate simulation, comparing collimated and focused 150 MeV electron beams.

Table 3. Percentage dose distribution for collimated and focused 150 MeV electron beams across different organs.

Organ	Angle	Percentage Dose Distribution (Collimated Electron 150 MeV) ± Uncertainty (%)	Percentage Dose Distribution (Focused 150 MeV Electron in 15 cm) ± Uncertainty (%)
Prostate	0°	99.2435 ± 0.0002	99.5721 ± 0.0003
	90°	53.4895 ± 0.0001	58.7387 ± 0.0003
	180°	99.2687 ± 0.0002	99.9021 ± 0.0003
	270°	62.1098 ± 0.0001	71.3257 ± 0.0003
Bladder	0°	0.2512 ± 0.0002	0.0751 ± 0.0002
	90°	43.8187 ± 0.0001	38.9457 ± 0.0001
	180°	0.2512 ± 0.0002	0.0733 ± 0.0002
	270°	37.4484 ± 0.0001	28.6487 ± 0.0007
RFH	0°	0.2315 ± 0.0002	0.0643 ± 0.0002
	90°	0.0732 ± 0.0003	0.0281 ± 0.0003
	180°	0.2313 ± 0.0002	0.0671 ± 0.0002
	270°	0.1216 ± 0.0002	0.0471 ± 0.0002
LFH	0°	0.2216 ± 0.0002	0.0641 ± 0.0002
	90°	0.0751 ± 0.0003	0.0261 ± 0.0003
	180°	0.2315 ± 0.0002	0.0635 ± 0.0002
	270°	0.1216 ± 0.0002	0.0487 ± 0.0002
Rectum	0°	1.0216 ± 0.0002	0.3414 ± 0.0002
	90°	3.3914 ± 0.0001	1.9812 ± 0.0007
	180°	0.2114 ± 0.0004	0.0484 ± 0.0005
	270°	0.3714 ± 0.0003	0.0552 ± 0.0005

Table 4. Mean percentage dose comparison for collimated and focused 150 MeV electron beams.

Organ	Mean Percentage Dose (Collimator) ± Uncertainty (%)	Mean Percentage Dose (Focused) ± Uncertainty (%)
Prostate	78.2865 ± 0.0001	82.3856 ± 0.0003
Bladder	20.3825 ± 0.0004	16.9365 ± 0.0004
RFH	0.1656 ± 0.0004	0.0565 ± 0.0001
LFH	0.1654 ± 0.0004	0.0564 ± 0.0001
Rectum	1.2465 ± 0.0002	0.6185 ± 0.0003

In Table 3, the dose distribution was calculated such that the sum of doses across all angles (0°, 90°, 180°, and 270°) for each organ equals 100 %. This approach ensures consistency in comparisons between collimated and focused beam setups. In Table 4, the reported values represent the mean dose received by each organ, averaged across all angles, and expressed as a fraction of the total dose delivered to the prostate. Although clinical practice often assesses dose coverage by the percentage of target volume receiving a specific percentage of the prescribed dose (e.g., 95 %), this approach ensures consistency in comparative dosimetric analysis between collimated and focused beams.

The Tables 3 and 4 and bar chart (Fig. 7) present detailed dose comparisons between collimated and focused beams across different organs, including the prostate, bladder, right femoral head, left femoral head, and rectum. The data

indicate that focused beams markedly reduce the dose to surrounding organs while maintaining high dose delivery to the prostate.

Statistical comparison of dose distributions between collimated and focused beams reveals significant differences, with the latter demonstrating a clear benefit. The normalized percentage dose data indicate that focused beams deliver a higher dose to the prostate while significantly reducing the dose to the bladder, rectum, and femoral heads. Specifically, the normalized dose to the prostate with focused beams is 82.38 %, compared to 78.28 % with collimated beams, representing a relative increase of 5.24 %. Conversely, the dose to the bladder is reduced from 20.38 % with collimated beams to 16.93 % with focused beams, representing a relative decrease of 16.93 %. The decrease in dose is even more pronounced for the right and left femoral heads, dropping from 0.16 % to 0.05 %, a reduction of 68.75 %. The rectum also benefits from a marked decrease in dose, from 1.24 % with collimated beams to 0.61 % with focused beams, representing a decrease of 50.81 %.

This analysis underscores the advantages of focused VHEE beams in radiotherapy. The decrease in scattering for focused beams leads to higher targeting accuracy, as demonstrated in our simulations. The focused beams not only achieve a higher dose to the prostate but also markedly reduce the dose to surrounding critical structures, such as the bladder, rectum, and femoral heads. This enhanced precision in dose delivery minimizes collateral damage to non-target tissues, highlighting the potential of focused VHEE beams to improve radiotherapy outcomes. The ability to spare healthy tissues while delivering a higher dose to the tumor makes focused VHEE a superior option for radiotherapy [27].

A comparison with previous study indicates that focused VHEE beams can deliver a concentrated dose to small volumetric elements within a target, with measured dose distributions aligning well with Monte Carlo simulations [7]. Similarly, Fan et al. (2023) highlighted the potential of focused VHEE beams to improve dose distribution by delivering high-dose concentrations to a small, well-defined spot with an extremely high dose rate [28]. Furthermore, research by Böhlen et al. (2024) supports the use of high-energy electron beams for their ability to achieve deep penetration and precise dose delivery, further validating the benefits of VHEE beams in radiotherapy [25].

Focused very high-energy electron (VHEE) beams have been optimized for radiotherapy using Monte Carlo simulations, demonstrating high precision and effectiveness in targeted treatments [29]. It further supports the conclusion that focused VHEE beams offer improved tumor targeting and better normal tissue sparing compared to conventional radiotherapy techniques.

The observed reduction in dose to surrounding organs can be attributed to the focused nature of VHEE beams. By confining the dose to a smaller, well-defined region, beam focusing reduces radiation spread, thereby minimizing exposure to adjacent tissues. This precise targeting capability is particularly beneficial for organs at risk near the treatment site. For instance, the significant reduction in dose to the bladder and rectum is especially important in prostate cancer treatment, as it may help lower the risk of radiation-induced side effects such as urinary and gastrointestinal complications.

CONCLUSION

This study highlights the significant advancements in radiotherapy achievable through the use of focused VHEE beams. The precision of focused VHEE beams demonstrates a marked improvement in dose delivery to the prostate, with 5.24 % higher doses compared to collimated beams, while effectively minimizing exposure to surrounding organs at risk. Specifically, the focused VHEE beams reduce the dose to the bladder, rectum, right femoral head, and left femoral head by 16.93 %, 50.81 %, and 68.75 % respectively, underscoring their superior precision and efficacy in targeting deep-seated tumors.

The implementation of a focused beamline using quadrupole magnets, along with the comprehensive dosimetric comparison, establishes a strong basis for clinical translation. These results advocate for the integration of focused VHEE beams into clinical practice, offering the potential for improved treatment outcomes and reduced side effects for patients undergoing radiotherapy for prostate cancer and other malignancies. Future work will focus on studying secondary particle production, such as neutrons, and conducting radiobiological studies using cell cultures.

ACKNOWLEDGMENT

AUTHOR CONTRIBUTION

E. M. Essaidi collected and analyzed the data, performed the simulations, wrote the first draft, and contributed to data interpretation. M. Krim and D. Benchekroun conceived the idea and supervised the work. O. Kaanouch assisted with data collection. M. O'Daniel contributed to the theoretical framework and provided the prostate data phantom. M. R. Mesradi supported data validation. All authors discussed, revised, and approved the final manuscript.

REFERENCES

1. D. Poppinga, R. Kranzer, W. Farabolini *et al.*, Biomed. Phys. Eng. Express **7** (2021) 015012.

2. A. Lagzda, D. Angal-Kalinin, J. Jones *et al.*, Nucl. Instrum. Methods Phys. Res. B **482** (2020) 70.

3. M. G. Ronga, M. Cavallone, A. Patriarca *et al.*, Cancers **13** (2021) 4942.

4. E. Schuler, E. Kjell, H. Elin *et al.*, Med. Phys. **44** (2017) 2544.

5. D. Poppinga, R. Kranzer W. Farabolini *et al.*, Biomed. Phys. Eng. Express **7** (2021) 015012.

6. L. Labate, D. Palla, D. Panetta *et al.*, Sci. Rep. **10** (2020) 17307.

7. K. Kokurewicz, E. Brunetti, A. Curcio *et al.*, Commun. Phys. **4** (2021) 33.

8. M. Bazalova-Carter, B. Qu, B. Palma *et al.*, Med. Phys. **42** (2015) 2615.

9. L. Whitmore, R. I. Mackay, M. van Herk *et al.*, Sci. Rep. **11** (2021) 14013.

10. T. T. Böhlen, J. -F. Germond, E. Traneus *et al.*, Med. Phys. **48** (2021) 3958.

11. L. Karsch, E. Beyreuther, O. Enghardt *et al.*, Acta Oncol. **56** (2017) 1359.

12. Z. Guo, S. Liu, B. Zhou *et al.*, arXiv:2312.03481 (2023) 1.

13. A. Sarti, P. De Maria, G. Battistoni *et al.*, Front. Oncol. **11** (2021) 777852.

14. H. El Bekkouri, E. Al Ibrahmi, M. El-Asery *et al.*, Atom Indones. **50** (2024) 135.

15. H. El Bekkouri, E. Al Ibrahmi, M. El-Asery *et al.*, Atom Indones. **50** (2024) 183.

16. T. E. Bakolia, A. Didi, R. Sebihi *et al.*, Atom Indones. **50** (2024) 37.

17. K. Kokurewicz, E. Brunetti, G. H Welsh *et al.*, Sci. Rep. **9** (2019) 10837.

18. J. Allison, K. Amako, J. Apostolakis *et al.*, Nucl. Instrum. Methods Phys. Res. A **835** (2016) 186.

19. B. Faddegon, J. Ramos-Méndez, J. Schuemann *et al.*, Phys Med. **72** (2020) 114.

20. C. Z. Jarlskog and H. Paganetti, IEEE Trans. Nucl. Sci. **55** (2008) 1018.

21. P. Arce and J. I. Lagares, Phys. Med. Biol. **63** (2018) 035007.

22. D. C. Hall and A. Makarova, H. Paganetti *et al.*, Phys. Med. Biol. **61** (2015) N1-N10.

23. J. O'Daniel, S. Das, J. Wu *et al.*, J. Phys.: Conf. Ser. **250** (2010) 012050.

24. E. Rodriguez, D. Skarecky, N. Narula *et al.*, The Journal of Urology **179 (**2008) 501.

25. T. T. Böhlen, J. -F. Germond, L. Desorgher *et al.*, Radiother. Oncol. **194** (2024) 110177.

26. D. E. Krim, A. Rrhioua, M. Zerfaoui *et al.*, Nucl. Instrum. Methods Phys. Res. A **1047** (2023) 167785

27. L. Whitmore, R. I. Mackay, M. van Herk *et al.*, Sci. Rep. **14** (2024) 11120.

28. D. Fan, Z. Liu, K. Fan *et al.*, *Characteristics of Focused Very High Energy Electron (VHEE) Beams in Radiotherapy, in:* Proceedings of the 14th International Particle Accelerator Conference (IPAC'23) (2023) 5179.

29. C. An, W. Zhang, Z. Dai *et al.*, Sci. Rep. **14** (2024) 79187.